

Photoisomerization of Azobenzenes and Spirocompounds in Nematic and in Twisted Nematic Liquid Crystals

Mariano L. Bossi,^{†,‡} Daniel H. Murgida,[§] and Pedro F. Aramendía^{*,†}

INQUIMAE and Departamento de Química Inorgánica, Analítica y Química Física, Facultad de Ciencias Exactas y Naturales, Universidad de Buenos Aires, Pabellón 2, Ciudad Universitaria, C1428EHA, Buenos Aires, Argentina, and Max-Volmer-Laboratorium, Institut für Chemie, Technische Universität Berlin, Sekr. PC14, Strasse des 17. Juni 135, D-10623 Berlin, Germany

Received: February 21, 2006; In Final Form: May 9, 2006

Samples of a nematic mixture of ZLI1132 and of a twisted nematic mixture composed of ZLI1132 and chiral inductor S811, including 1%–10% (w/w) 4-*N,N*-dimethylaminoazobenzene (DAB), (4'-nitro)-4-*N,N*-dimethylaminoazobenzene (NDAB), spiropyran (SP), or spirooxazine (SO) were irradiated to produce the photochromic transformation of the dopant. The changes in the system were monitored by time-resolved transmission spectroscopy, time-resolved birefringence, or polarized Raman scattering. The medium sensitivity of the kinetics and spectroscopy of some of the probes was used to derive information on polarity of the medium. In the systems studied, apart from the changes in absorption spectrum, great changes in birefringence can be photoinduced and the order of the nematic phase can be changed in either direction, depending on the dopant. The open form of SP can discriminate orientation polarity. Although the polarity parallel to the mesogenic director is similar to that for acetone, the perpendicular orientation has a polarity similar to acetonitrile. In agreement with this observation, the kinetics of the *Z* → *E* isomerization of NDAB, oriented parallel to the mesogenic director, also experiences a polarity similar to that for acetone. The decay rate constant of the open form of SP displays a linear relationship between its Arrhenius parameters, which is universal in a great variety of homogeneous solvents, solvent mixtures, and liquid crystals, therefore validating the hypothesis that the same type of transformation is observed in all these cases, namely, the decay of the open form monomer. The dopants used have been proven to be adequate probes of bulklike properties in locally heterogeneous systems as liquid crystals.

Introduction

Since their discovery over 100 years ago, liquid crystals have attracted considerable attention, because of their unique properties of fluidity and relatively high molecular order.¹ Their use in displays of portable computers and phones is a practical realization that takes advantage of these special features. Photoinduced changes of the liquid crystal properties and state offer the possibility of wireless control of such devices. Many systems have been investigated in which the light active moiety was either dissolved in the liquid crystal, incorporated to the mesogenic molecule, or even was part of the commanding layer of surface-induced alignment cells.^{2–7} Observed photoinduced effects include changes of molecular order, phase, pitch, birefringence, polarization, or circular dichroism.^{8–14}

Photochromic molecules are bistable systems that can be interconverted by light, heat, or both.^{15,16} This property makes these molecules ideal for the design of memories and switches.¹⁷ When the photochromic transformation is accompanied by a great change of molecular geometry between the two photochromic forms, then the possibility of photoinduced changes can be enhanced by the susceptibility of the mesogenic phase

to the molecular shape of the guest. This is the basis of the observed effects in the great majority of the systems studied.

Azobenzenes (ABs), which photoisomerize from a stable *E* form to a metastable *Z* form via visible light, have been widely used for these purposes.^{18–20} The *Z* isomers of ABs return thermally to the *E* form with a rate constant that spans more than 6 orders of magnitude, depending on the relative order of the *n*– π^* and π – π^* excited states.^{21,22} Because of the existence of an inversion reaction pathway in parallel to the *N*–*N* rotation pathway, ABs efficiently isomerize, even in constrained media. Furthermore, the thermal reaction of *push*–*pull* pseudo-stilbenoids is greatly influenced by the polarity of the environment.^{23,24} The lower affinity of the bent *Z* form for rodlike mesogenic molecules, compared to the extended *E* form, efficiently induces big medium changes that accompany the photochromic transformation.

Spiropyrans (SPs) and spirooxazines (SOs) (see Scheme 1) can also experience an efficient photochromic transformation via C–O cleavage upon near-UV irradiation.^{25–27} This bond breaking transforms the stable spiro form to an open form structure, merocyanine (MC) that has extended conjugation and displays a strong absorption in the green region of the spectrum. The MC form thermally reverts to the closed stable isomer. For SP, the absorption spectrum of the open MC form displays a negative solvatochromism²⁸ and the rate of the back thermal reaction is strongly influenced by the medium polarity.^{28–30} In contrast to AB, the MC photoisomer of both SP and SO, which

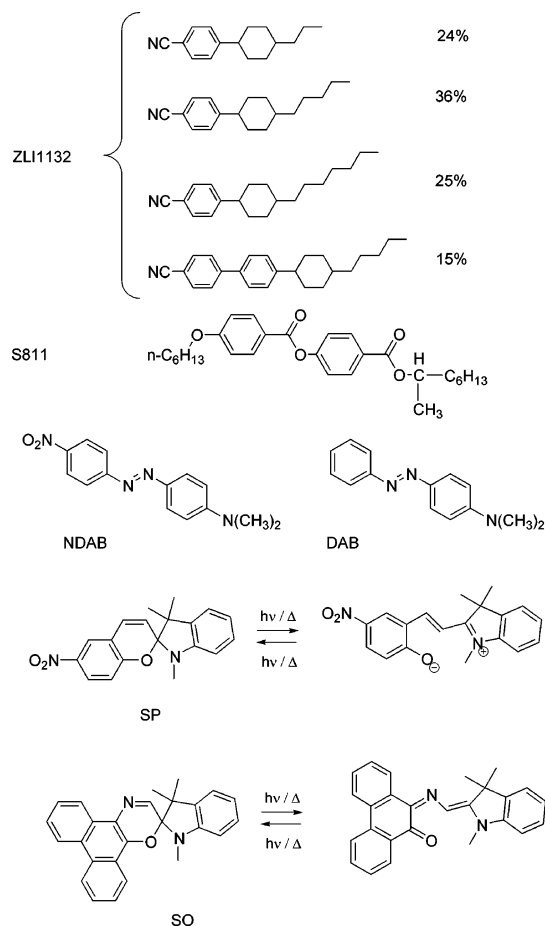
* Author to whom correspondence should be addressed. Fax: 54 11 4576 3341.

[†] Universidad de Buenos Aires.

[‡] Present address: Department of NanoBiophotonik (200), Max Planck Institute for Biophysical Chemistry, Am Fassberg 11, 37077 Göttingen, Germany.

[§] Technische Universität Berlin.

SCHEME 1: Structure of the Components of the Nematic Liquid Crystal Mixture ZLI1132, the Chiral Inductor S811, and the Photochromic Systems Used



is due to the all-trans polymethine chain, has a more-rodlike shape than that of the stable closed form.

In this work, we investigate nematic and twisted nematic liquid crystals mixed with AB, SO, and SP by spectroscopic methods, including birefringence and polarized transmission, to monitor the amplitude of the changes upon phototransformation as well as the dark kinetics. We take advantage of the appointed environment sensitivity of the kinetics to determine local polarity and to discern differences in polarity according to the direction in surface-induced oriented nematic samples. In addition, we measure the polarization ratios of characteristic Raman active bands to prove that SO orders the nematic medium upon conversion to the open form.

Experimental Section

Materials. 1',3'-Dihydro-1,3,3-trimethyl-6-nitrospiro[2H-1-benzopyran-2,2'-(2H)-indoline] (SP) (Aldrich), 2,3-dihydro-1,3,3-trimethylspiro[indoline-2,2'-(2H)phenanthro[9,10b][1,4]oxazine] (SO) (Aldrich), 4-(*N,N*-dimethylamino)azobenzene (DAB) (Aldrich), commercial liquid crystal mixture ZLI-1132 (Licristal/Merck), and chiral inductor S-811 (Licristal/Merck) were used as supplied. 4-(*N,N*-Dimethylamino)-4'-nitroazobenzene (NDAB) was synthesized according to standard procedures for azo dyes by mixing *p*-nitroaniline with NaNO_2 and a later addition of *N,N*-dimethylaniline. The crude reaction mixture was purified by column chromatography (ethyl acetate:hexane 5:95), and its purity was checked by thin-layer chromatography (TLC) and nuclear magnetic resonance (NMR) (^1H NMR, 200 MHz, CDCl_3 , δ 3.13 (s 6H, $\text{N}(\text{CH}_3)_2$), 6.76 (d 2H, $J = 9.3$ Hz, H3),

7.91 (d 2H, $J = 9.3$ Hz, H2), 7.92 (d 2H, $J = 9$ Hz, H2'), 8.32 (d 2H, $J = 9$ Hz, H3')). Cells of parallel polyimide rubbed layers, spaced 2, 4, and 10 μm apart and coated with indium tin oxide (ITO), which were used for dichroism and birefringence measurements, were purchased from E.H.C. Co., Ltd. (Japan).

Sample Preparation. Nematic mixtures of ZLI-1132 and dyes with different compositions were prepared by weighting each component and then stirring the mixture for at least 6 h at ~ 40 – 50 $^\circ\text{C}$ in the dark. The typical composition of the mixture was $\sim 5\%$ w/w in the probe. Cells were filled at room temperature by the capillary effect, and the orientation was verified by polarized microscopy. Twisted nematic liquid crystals were prepared by stirring overnight weighted mixtures of ZLI-1132 and S-811 at room temperature. This chiral inductor is known to induce a left-handed helical structure with a helical twisting power (HTP) of $-13.9 \mu\text{m}^{-1} \text{M}^{-1}$ in this nematic mixture.³¹ These mixtures, when oriented, present a Grandjean or planar texture in a microscope between crossed polarizers and a reflection band is observed by ultraviolet–visible (UV–Vis) transmission spectroscopy. The amount of the inductor was adjusted to 15%–20% (w/w) to place this reflection band in the red or near-infrared (NIR) range, far enough from the absorption bands of the stable dyes and of their metastable photoisomers. Guest–host twisted nematic samples were prepared in the same way as the nematic samples, and in similar final composition of the probe. Persistence of the mesophase was verified by polarized microscopy and UV–Vis spectroscopy, and a pitch modification was observed by transmission spectroscopy compared to the pure twisted nematic mixture, mainly because of the effect of dilution of the chiral inductor.

Parallel and perpendicular directions of nematic samples are referred to the sample orientation director. In the case of twisted nematic samples, parallel and perpendicular directions are referred to the microscopically local sample's director.

Instrumentation. Dichroism measurements were performed in a Hewlett–Packard UV–Vis diode array spectrophotometer (model HP-8452A) with a film polarizer placed before the sample, as described previously.³²

Birefringence measurements were performed by placing the sample between polarizers and measuring laser light of 785 nm transmitted by the system in the setup described in a previous work.³²

Raman spectra were measured in backscattering geometry using a microscope that was coupled to a single-stage spectrograph (Jobin Yvon, model LabRam 800 HR) that was equipped with charge-coupled device (CCD) detection. Elastic scattering was rejected with super Notch filters. The 514-nm line of a continuous wave (cw) argon ion laser (Coherent Innova 300) was passed through a polarizer and a polarization rotator and then focused onto the sample by means of a long-working-distance objective (20 \times ; N.A. = 0.35).

Typically, experiments were performed with laser powers of ca. 1 mW at the sample, effective acquisition times of 5 s and spectral resolution of 2 cm^{-1} .

The samples were positioned on the microscope table with the director axis either parallel or perpendicular to the polarization axis of the laser. The collected scattered light was passed through an analyzer that was oriented parallel to the laser polarization and a scrambler before entry to the spectrograph.

Samples for Raman measurements were prepared in the same manner as that described for dichroism and birefringence.

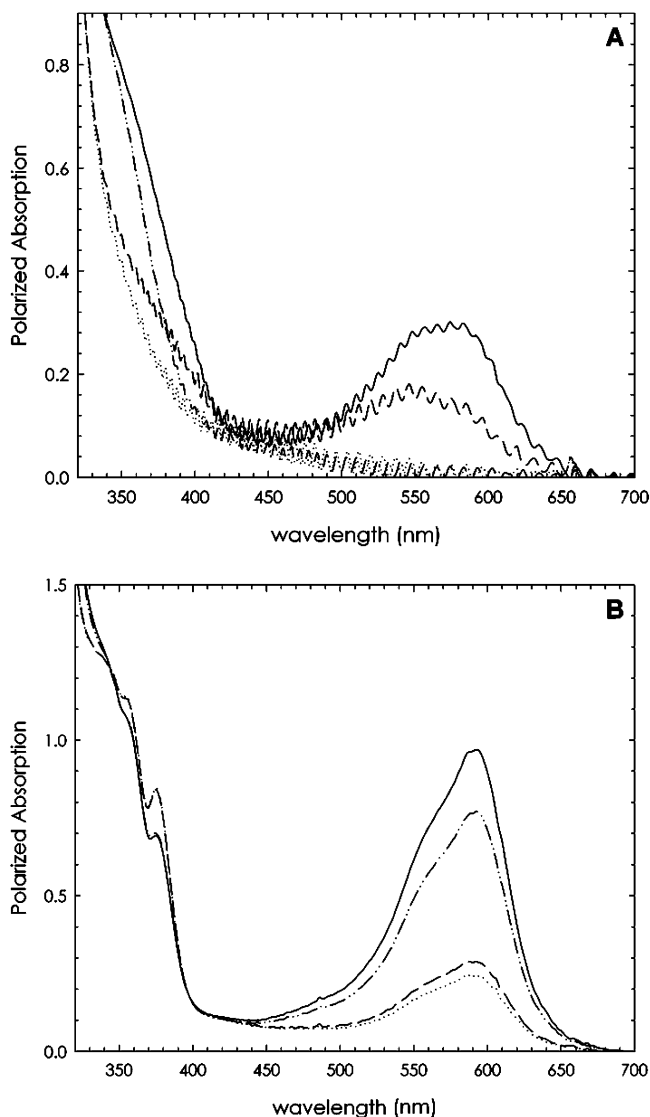


Figure 1. (A) Polarized absorption spectra of SP 6.4% w/w in ZLI ($d = 10 \mu\text{m}$) before irradiation with a flash of light (UG11 filter) (— · · —) parallel spectrum and (— · —) perpendicular spectrum) and after irradiation with a flash of light (UG11 filter) (—) parallel spectrum and (---) perpendicular spectrum). (B) Spectra taken under the same conditions for a sample of 4.9% w/w SO in ZLI ($d = 10 \mu\text{m}$) (the same curve style code as that in Figure 1A was used in Figure 1B).

Results

Nematic Phase. Both SP and SO exhibit photoconversion to the corresponding MC when included in nematic and twisted nematic phases. In the case of SO, there is a detectable amount of the open MC form in thermal equilibrium, even at room temperature, as it was observed in common solvents.^{33,34} Polarized absorption spectra of samples of SP and SO in the nematic phase before and after irradiation with UV light are shown in Figure 1. The values of the dichroic ratio (d), which is defined as the ratio between parallel and perpendicular polarized absorption ($d = A_{\parallel}/A_{\perp}$), show that the MC form, because of its rodlike shape, has a high degree of order in the LC and that, for both SP and SO, it orients preferably parallel to the nematic director (see Table 1). The electronic absorption band in the visible of the MC forms is originated in a $\pi \rightarrow p^*$ transition, which has a transition moment along the polymethine chain. It is important to notice that order parameters are higher for SO than for SP, both before and after irradiation, but the change is more pronounced for SP. This can be due to the higher

TABLE 1: Dichroic Ratios in Nematic Phase

compound	concentration (% (w/w))	wavelength (nm)	d_{before}	d_{after}	conversion
SP	6.4	380Å	1.25	1.9	3 ^a
SP	6.4	560		1.9	
SO	4.9	374	0.83	0.83	1 ^{a,b}
SO	4.9	590	3.2	3.4	
NDAB	0.9	490	6.2	3.9	>22 ^c

^a Calculated assuming the same absorption coefficient for the MC form as in solution. Reference 52 was used for SP, and reference 48 was used for SO. ^b Difference in conversion, calculated from the amount of the closed isomer in the photostationary state and in the initial state, respectively. ^c Minimum limit estimated assuming that the Z isomer does not absorb at 490 nm.

conversion attained with SP upon irradiation, because of the longer lifetime of its MC photoisomer.

Polarized Raman measurements were performed to detect the off-resonance signals of the mesogenic molecules. The bands detected correspond to CN stretching (2225 cm^{-1}), aromatic ring stretching (1605 cm^{-1}), and C-phenyl stretching (1177 cm^{-1}).^{35,36} All these transitions have the greatest polarization tensor component parallel to the long molecular axis.^{37,38} The polarized Raman spectra are shown in Figure 2 for a ZLI mixture containing SO in darkness (Figure 2A) and under continuous irradiation in the UV (Figure 2B). Figure 2C shows the ratio of intensities of the Raman scattering bands when the irradiation is parallel and when it is perpendicular to the orientation director of the nematic phase. Four series of data are shown vertically. The leftmost data series of Figure 2C corresponds to the pure ZLI phase. The second and fourth series correspond to the SO-doped ZLI mixture in darkness, whereas the third series corresponds to the same mixture under steady-state irradiation in the UV range. Clearly, the polarization ratio of the Raman lines of the mesogen mixture increases consistently upon irradiation, and returns to the darkness value when the light is turned off (rightmost data). Under UV irradiation of SO, polarization ratios similar to those for the pure ZLI phase are obtained. Similar experiments with SP were not successful, because of photodecomposition of the dopant.

The MC form of SP shows different absorption energy for parallel and perpendicular orientation in the nematic phase (orientation solvatochromism). Absorption spectrum and lifetime of the MC of SP are known to be sensitive to the polarity of the medium. Thus, the observed shift is an indication that this probe is sensing different environments, depending on the orientation in the absorption time scale ($<1 \text{ fs}$). Normalized difference absorption spectra displayed in Figure 3 show a maximum of absorption at 550 nm for perpendicular orientation (similar to acetonitrile, 553 nm) and at 567 nm for parallel orientation (similar to that for acetone, 565 nm).^{28,39}

The dichroism of NDAB in the nematic phase in darkness is also very high when the molecule is in its E conformation (see Table 1). The higher dichroic ratio of NDAB, compared to that of similar compounds (azobenzene and 4-(*N,N*-dimethylamino)-azobenzene), is not only a result of the better alignment of the transition dipole with the long molecular axis, because of its extended conjugation, but also of a better alignment of the molecule in the nematic phase. The order of the nematic layer is highly disturbed upon buildup of the Z isomer, and the dichroic ratio (at 490 nm) decreases from 6.2 to 3.9 after flash excitation.

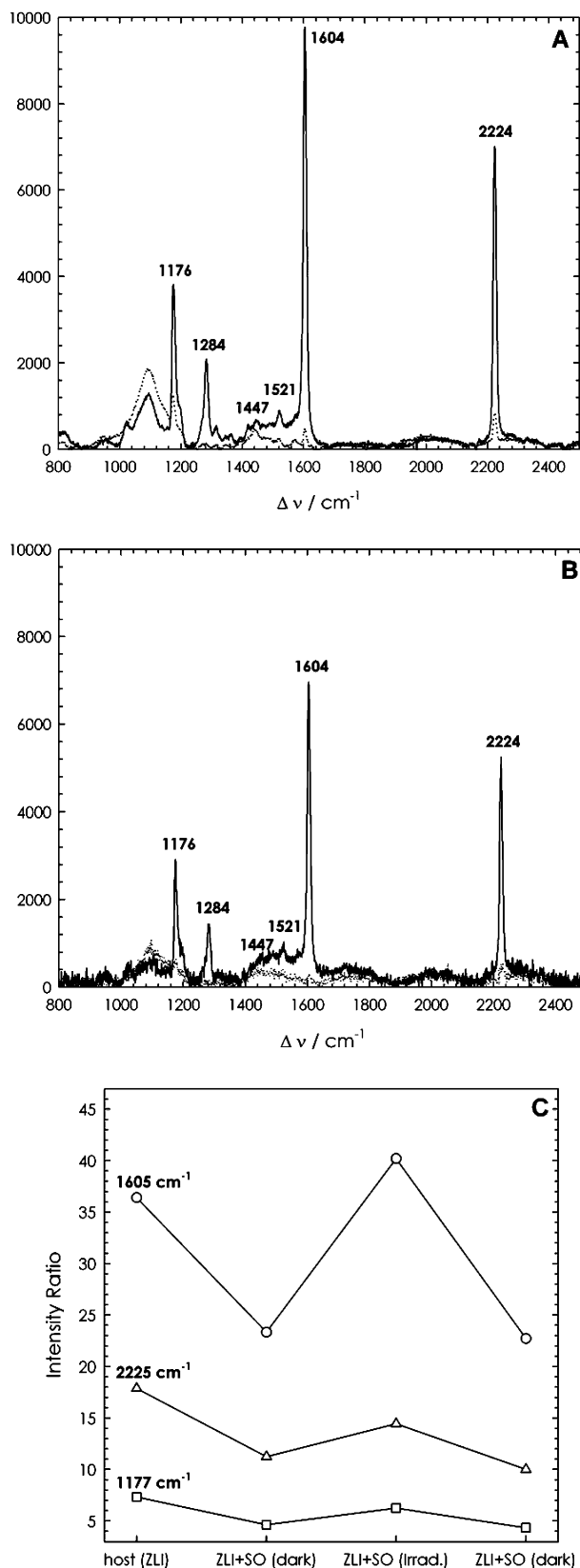


Figure 2. Polarized Raman spectra of a sample of SO (3.7% w/w) in ZLI 1132, excited at 514 nm (1 mW): (A) no UV background irradiation (the sample director was placed parallel (full line) or perpendicular (dotted line) to the excitation and detection direction); (B) under steady-state UV irradiation with a xenon arc lamp and a BG4 filter (two spectra recorded under the same conditions as in Figure 2A); and (C) polarized intensity ratio of parallel and perpendicular spectra for the bands at (○) 1605 cm^{-1} , (△) 2225 cm^{-1} , and (□) 1177 cm^{-1} .

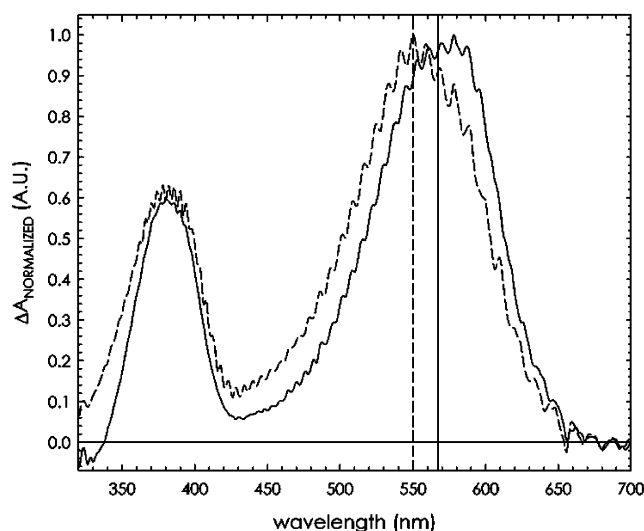


Figure 3. Difference absorption spectra of a sample of 6.4% w/w SP in ZLI ($d = 10 \mu\text{m}$) after and before irradiation with a flash of light (UG11 filter), normalized to their correspondent maximum; the difference spectra obtained (---) perpendicular (dashed line) and (—) parallel to the nematic director are shown.

The kinetics of the thermal back isomerization ($\text{MC} \rightarrow \text{SP}/\text{SO}$) was investigated in the nematic phase as a function of temperature. Thermal decay after irradiation was followed at the absorption maxima of the corresponding MC form for both components of the polarized spectra. Monoexponential behavior was observed for SO, whereas the decay kinetics for SP was fitted to a sum of two exponential terms. The same lifetimes are obtained at every temperature for the parallel and for the perpendicular components. This is compatible with a probe that changes orientation fast during its lifetime and an intrinsic biexponential decay of the MC form of SP, as already observed in other media, especially in alcohols.^{39,40} The results of these experiments are summarized in Table 2 for both probes in the nematic phase. Table 3 summarizes the corresponding Arrhenius parameters. For SP, higher activation energy and entropy values than those measured in any common fluid medium are obtained.

The lifetime of the Z isomer of NDAB was also measured as a function of temperature in the nematic phase (see Table 2). This lifetime is highly dependent on the polarity of the medium.^{23,24,41} A good correlation between the activation free energy for the decay of this isomer and the solvent parameter $E_T(30)$ is obtained for nonprotic solvents. This correlation can be represented by the line $\log[k(\text{s}^{-1})] = 0.36 \times E_T(30)$ (kcal/mol) + 14.2, based on literature data.⁴² The decay rate constant of NDAB in the nematic phase at 25 °C (5.8 s^{-1}) corresponds to an $E_T(30)$ value of 41.5 kcal/mol, which is slightly smaller than the value for acetone.⁴³ The polarity deduced from this measurement is in agreement with that deduced from the position of the absorption of the MC form of SP. The activation parameters for the $\text{Z} \rightarrow \text{E}$ isomerization of NDAB in the nematic phase are shown in Table 3. The activation energy of 45 kJ/mol is comparable to the value measured in acetone⁴¹ and is smaller than the value reported in other nonpolar solvents.^{41,44} The activation entropy is negative, and its absolute value is also greater than the values reported in nonpolar solvents.

Birefringence measurements were attempted with samples of SO and SP under similar flash photolysis energy as for the dichroism experiments, but no change in the transmission of the sample placed between polarizers could be detected. Light

TABLE 2: Rate Constants for the Dark Decay of the Photochromic Systems after Light Pulse Irradiation, as a Function of Temperature in the Nematic and in the Twisted Nematic Phases

probe	Nematic				Twisted Nematic			
	concentration (% w/w)	temp. T (°C)	k_1^a (s ⁻¹)	k_2^a (s ⁻¹)	concentration (% w/w)	temp. T (°C)	k_1^a (s ⁻¹)	k_2^a (s ⁻¹)
SP					6.0 (17.6% w/w S811)	19.7	5.88×10^{-3}	1.70×10^{-3}
SP	6.0	28.3	5.62×10^{-3}	1.53×10^{-3}	6.0 (17.6% w/w S811)	29.3	1.56×10^{-2}	6.53×10^{-3}
SP	6.0	38.4	2.24×10^{-2}	7.1×10^{-3}	6.0 (17.6% w/w S811)	38.9	4.1×10^{-2}	2.13×10^{-2}
SP	6.0	47.8	1.05×10^{-1}	3.34×10^{-2}	6.0 (17.6% w/w S811)	48.8	1.38×10^{-1}	5.7×10^{-2}
SP					6.0 (17.6% w/w S811)	58.7	4.5×10^{-1}	2.4×10^{-1}
SO	6.1	20.8	7.9×10^{-2}		5.7 (16.7% w/w S811)	20.0	3.13×10^{-2}	
SO	6.1	29.3	2.06×10^{-1}		5.7 (16.7% w/w S811)	29.9	8.8×10^{-2}	
SO	6.1	37.9	4.8×10^{-1}		5.7 (16.7% w/w S811)	39.5	2.4×10^{-1}	
SO	6.1	46.7	1.1×10^0		5.7 (16.7% w/w S811)	44.4	4.2×10^{-1}	
SO					5.7 (16.7% w/w S811)	54.3 ^b	1.3×10^{0b}	
NDAB	0.9	15.1	3.83×10^0		0.5 (17.4% w/w S811)	21.8	3.53×10^0	
NDAB	0.9	24.9	5.88×10^0		0.5 (17.4% w/w S811)	29.9	6.13×10^0	
NDAB	0.9	42.2	1.7×10^1		0.5 (17.4% w/w S811)	38.7	9.4×10^0	
NDAB	0.9	51.2	3.4×10^1		0.5 (17.4% w/w S811)	46.7	1.61×10^1	
NDAB	0.9	64.9	5.9×10^1		0.5 (17.4% w/w S811)	56.1 ^b	2.5×10^{1b}	

^a Uncertainty in the rate constants is $\pm 20\%$. ^b Isotropic phase.

TABLE 3: Arrhenius Parameters of the Rate Constants of Table 2^a

	Nematic		Twisted Nematic		Solvents	
	E_a (kJ/mol)	ΔS^\ddagger (J/(mol K))	E_a (kJ/mol)	ΔS^\ddagger (J/(mol K))	E_a (kJ/mol)	ΔS^\ddagger (J/(mol K))
SP						
k_1	120 \pm 9	+103 \pm 8	90 \pm 4	+10 \pm 1	71–105	-39/+50
k_2	127 \pm 5	+114 \pm 5	100 \pm 4	+35 \pm 1	71–105	-39/+50
SO	80 \pm 1	-4 \pm 1	82 \pm 2	-3 \pm 1	66–72	-47/-23
NDAB	45 \pm 2	-89 \pm 4	46 \pm 1	-87 \pm 2	45–64	-16/-31
DAB	52 \pm 3	-113 \pm 40	52 \pm 3	-100 \pm 7	88	-11

^a The values for DAB in the nematic phase³² are given for comparison.

of a higher power was used to achieve higher conversion of the sample. Thus, after 2 s of irradiation with a high-pressure mercury lamp and a 2-mm BG3 filter (150 mW at 360 nm) or after 30 pulses with a frequency-tripled Nd:YAG laser (355 nm, 10 Hz, 20 mJ/pulse, 8 ns full width at half maximum, fwhm), a change in birefringence was observed for both SO and SP. After dark relaxation of the system, the initial state was recovered. Reproducibility was observed for SO after ca. 50 irradiation cycles, but SP showed decomposition (permanent bleaching) after a few cycles.

For SO, transients of the transmitted light were recorded at different fixed analyzer orientations and the polarization ellipse was reconstructed at every time after photoconversion. Figure 4 shows the transients of the parameters characterizing the emerging polarization ellipse after photolysis of a sample of SO in nematic phase at 15 °C. Data were fitted assuming a monoexponential behavior of the optical delay (δ) with time, according to eq 1.

$$\delta(t) = \Delta\delta_0 \exp\left(-\frac{t}{\tau}\right) + \delta_\infty \quad (1)$$

The relationship between the birefringence of the nematic phase (Δn), δ , and the parameters of the polarization ellipse are shown in eqs 2 and 3, respectively:

$$\delta = \frac{2\pi(\Delta n)l}{\lambda} \quad (2)$$

$$\tan(2\Psi) = \tan(2\beta) \cos(\delta) \quad (3a)$$

$$\sin(2\chi) = \sin(2\beta) \sin(\delta) \quad (3b)$$

where Ψ is the angle between the major axis of the polarization

ellipse and the laboratory fix vertical axis and χ is the angle characterizing the ellipticity of the light transmitted by the sample. In eq 2, λ is the wavelength of the probing laser (785 nm), and l is the thickness of the nematic sample. In eqs 3, β is defined as the angle formed by the nematic director and the plane of polarization of the incident light (30° in our experiments). The time-dependent parameters that characterize the polarization ellipse, which were fitted according to eqs 1 and 3, are plotted together with the data in Figure 4, and residuals are shown in the upper plot of the same figure. A monoexponential decay with lifetimes of 0.084 s⁻¹ at 15.6 °C, and 0.43 s⁻¹ at 28.6 °C describes the birefringence time dependence with a good precision.⁴⁵ These values are higher than those obtained from dichroism for the same system (see Table 2). The difference can be well explained by the higher conversion needed to perform these measurements.

After the photolysis of NDAB, much-greater changes in birefringence are observed than for either SP or SO, indicating a greater perturbation of the nematic phase. As a comparison, maximum birefringence amplitudes ($\Delta\delta_0$) of 4°–5° can be obtained in samples that contain 6% w/w SO under 50%

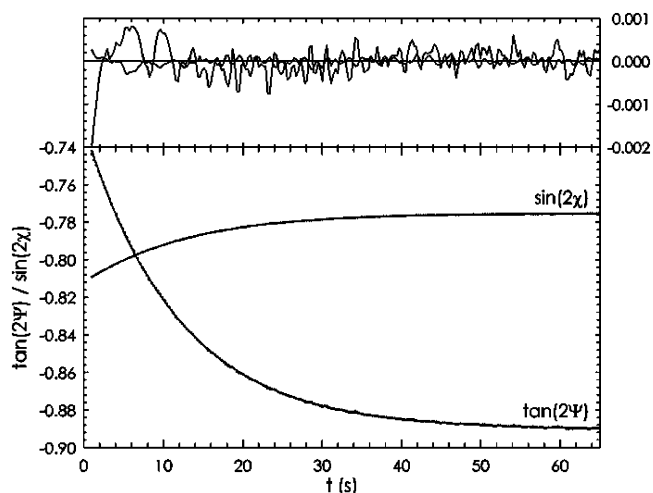


Figure 4. Time dependence of the polarization ellipse parameters (eqs 1–3 of the text) emerging from the cell after photolysis of a 6.1% w/w SO in ZLI1132 sample at 354 nm under the conditions specified in the text (ca. 50% conversion to the MC photoisomer) at 15 °C. Experimental data (dots) and fitting curves according to eq 1 and 3 of the text (full lines) are shown in the main plot, and the upper plot contains the residuals of this fit.

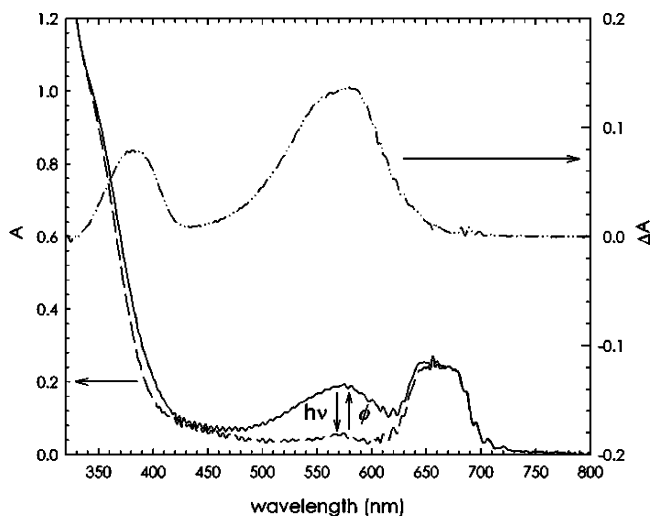


Figure 5. Absorption spectra (---) before and (—) after UV flash irradiation of a 6.0% w/w SP sample in a twisted nematic mixture of ZLI1132 with 17.6% w/w S811 (left axis). The upper spectrum (dashed dotted line) represents the difference absorption between after and before irradiation (right axis).

conversion to the photoisomer, whereas changes up to 8° can be obtained upon 20% conversion of a 0.9% w/w NDAB-containing nematic sample. For NDAB, the amplitude of the change in birefringence increases as the clearing point is approached.

Decay rate constants for the photoisomer obtained as explained previously at different temperatures and activation parameters were similar to those obtained in dichroism measurements (see Tables 2 and 3). For NDAB, the conversion was similar in both types of experiments.

Twisted Nematic Phase. Inclusion of up to 6% w/w SO or SP into twisted nematic mixtures of ZLI1132–S811 (up to 19% w/w of this chiral inductor in the mesogenic mixture) shows persistence of the mesophase, as verified by polarized microscopy. Under these conditions, SO and SP show similar photochromic behavior as observed in the nematic phase. Colorability and bleaching processes are reproducible at least under low-power pump conditions. SO shows ca. 1% open form in thermal equilibrium at 20°C in darkness, similar to the behavior in the nematic phase.

The reflection band of the twisted nematic phase was monitored at its maximum when samples of SO and SP were irradiated. For samples up to 6% w/w of the probe, no change in the position or the shape of this band was observed, even at the photostationary state (i.e., high conversion). In Figure 5 spectra are shown for a sample of SP 6% w/w before and after irradiation as well as the difference spectrum for 2% of conversion.

Thermal back isomerization was recorded at different temperatures for both probes in the twisted nematic phase. Kinetics of the bleaching reaction was followed at the absorption maxima of the corresponding MC. As in the nematic phase, the decay of the MC form of SP is a sum of two exponential terms, whereas the decay of the MC form of SO is monoexponential. The activation energy and entropy of the two components of the MC decay of SP are lower than those in the nematic phase. The Arrhenius parameters for the decay of the MC form of SO are equal to those measured in the nematic phase. Results are summarized in Table 3.

The thermal $Z \rightarrow E$ isomerization of NDAB and DAB was also monitored in samples that contained the dyes in proportions of <1% w/w and up to 6% w/w, respectively, with respect to

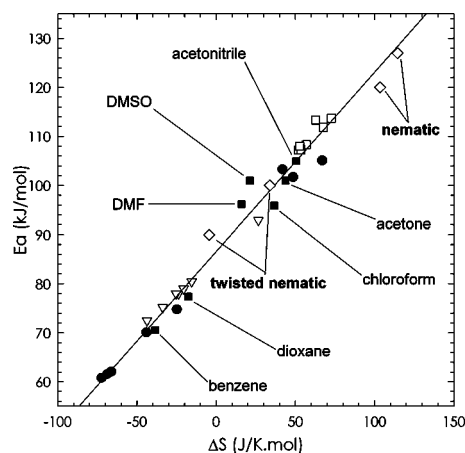


Figure 6. Correlation of the activation parameters of the thermal decay of the MC isomer of SP in different media. The line represents the best linear fit with a slope of 365 K: (■) neat solvents,^{25,28,29,40} (●) toluene–acetonitrile mixtures,³⁹ (▽) hexanes–ethanol mixtures (fast component),³⁹ (□) hexanes–ethanol mixtures (slow component),³⁹ and (◇) mesogenic phases (this work).

the twisted nematic mixture (up to 20% w/w of S811). No perturbation was observed in the reflection band upon photolysis of NDAB, and slight changes were registered in this band for DAB systems, which decayed with the same kinetics as the changes in the absorption band of the azobenzene. The thermal $Z \rightarrow E$ isomerization is monoexponential in both cases with similar activation energy and entropy as in the nematic phase.³² The kinetic results are summarized also in Table 3.

Discussion

Results will be analyzed from two points of view: On one hand, considering the effect of the host on the photochromic system, especially on the thermal back isomerization reaction. On the other hand, regarding the photoinduced changes produced by the photochromic probes included in the mesophases, with the interest focused on bistable photoinduced systems.

Regarding the influence of the medium on the cyclization reaction of spirocompounds, attention must be centered on the activation parameters. Comparison with values observed in common solvents indicates that a much-higher activation energy and a more-positive activation entropy are obtained in liquid crystals, with the effect being more important for SP than for SO. The same fact was observed by Otruba and Weiss in smectic phases, compared to the isotropic phase of the same mesogen.⁴⁶ In Table 3, a comparison of the values of the Arrhenius activation parameters for both mesophases is made with values in selected solvents. Activation energy and activation entropy are highly correlated for the ring closure of the MC form of SP in a variety of media. The Arrhenius parameters of the nematic and twisted nematic phases fit very well in this correlation,³⁹ as illustrated in Figure 6. The slope of this plot is 365 K, which is very different from the average temperature of 310 K of the measurements, ensuring that the correlation is not an artifact that results from the Arrhenius-type fitting of the rate constants.⁴⁷ The activation energy and entropy in the nematic phase are higher than all the values reported in isotropic solvents, but they are smaller than the values reported by Otruba and Weiss in the smectic phase of *n*-butyl stearate.⁴⁶ These high values reflect the energy and entropy differences involved in rearranging the environment of the mesogenic phase to accommodate the biradicaloid and more-global transition state, compared to the dipolar, extended, and more-rodlike MC.^{29,30} The values of the

activation parameters are smaller in the twisted nematic phase, because of the lowering of order and polarity that is caused by the presence of the chiral inductor. The fact that all the measured rate constants fit in the same correlation favors the assignment to the same type of process, namely accommodation of the extended polymethine chain to form the globular transition state for ring closure. This is achieved by C–C bond twist. An important difference of the behavior observed in alcohols, with respect to mixtures of alcohols and other solvents and to the mesophases should be emphasized: in neat alcohols, only the smaller rate constant of the biexponential decay fits into the correlation of Figure 6 (data not included in the figure), whereas in ethanol–hexane mixtures and in the mesophases, both constants are in the correlation.^{39,40}

The decay of the MC form of SO is not influenced very much by the environment.⁴⁸ This is due to the more covalent (quinoid) nature of the open form,⁴⁹ as well as to the presence of a N atom in the conjugated chain that provides an inversion pathway for reorganization of this chain to rebuild the closed form.

On the other hand, for azobenzenes, the activation energy takes values comparable to the smallest values observed in common liquids.^{41,44,46} For this probe, the inversion mechanism of the $Z \rightarrow E$ isomerization has a transition state with a rodlike shape, with a greater affinity for the mesophase than the bent Z form.^{44,46} This explains also the high absolute value of the negative activation entropy. Results previously published for DAB³² in the same mesophases are consistent with this explanation.

SP presents a particular case among the three probes studied in this work. On one hand, the decay of the open form is biexponential with identical lifetimes for the two polarized absorption directions. On the other hand, there is an important shift between polarized components of the visible absorption band of the MC form of SP.

The difference between the isotropic kinetic behavior and the anisotropy of the absorption spectra can be explained by the different time scales in which the two processes occur. In the 10^0 – 10^3 s time scale, the probe can reorient rapidly and average all orientations in the mesophase, so that decay probed in any direction is equivalent. In contrast, on the light absorption time scale, the molecules are frozen in their orientation, with respect to the mesophase director, and, thus, experience anisotropic effects that can be rationalized, considering that the polarization is a tensor.⁵⁰

The polarity sensed by MC is higher in the perpendicular orientation, with polarity ranging from that of acetone to that of acetonitrile. To support this evidence, and considering that the absorption energy of the MC form correlates linearly with the thermal activation free energy of the decay rate constant,²⁸ we studied the reaction in acetone at similar concentration and conversion as in the mesophases. We observed a monoexponential behavior with the same lifetime informed in bibliography for diluted solutions of SP in acetone ($k^{298\text{K}} = 7.22 \times 10^{-3} \text{ s}^{-1}$).²⁸ The previous discussion is further supported by the polarity similar to that of acetone sensed by the $Z \rightarrow E$ isomerization of NDAB. This later probe has a preferential orientation parallel to the nematic director, and, therefore, the result matches the acetone-like environment sensed by the parallel orientation of MC.

Dichroism experiments suggest that, for both spirocompounds, the photoconversion to the open form is accompanied by an increase in the order of the nematic phase, as evidenced by the increase in the dichroic ratio of the MC form in the visible. Dichroism experiments measure the average orientation

of the direction of the electronic transition dipole, with respect to the director of the mesophase. When comparing dichroic ratios of two different compounds, one must consider two factors: the orientation of the transition dipole, relative to the molecular axes, and the orientation of these axes, relative to the nematic director.⁵¹ The molecule orients in the monodomain-ordered mesophase according to its aspect ratio, and thus dichroism is an indirect measurement of the nematic order. A direct measure of the order of the mesogen molecules is provided by the polarization of its Raman bands, as illustrated in Figure 2. As Figure 2C shows, all three bands with polarization ellipse with the largest component along the mesogenic long molecular axis, increase its parallel intensity, with respect to the perpendicular intensity, upon photoisomerization of SO to the MC form. This change is consistent in the three bands considering that the ratio of polarization between any chosen pair of bands is constant before and after irradiation. Exception is the band at 1605 cm^{-1} after irradiation. This deviation can be explained because of small variations in the intensity of the perpendicular spectrum that have a great influence in the value of the polarization ratio. From these experiments, we can safely ensure that there is an increase in the order of the mesogenic molecules after photoconversion of SO to the open MC form. This probably is also the case for the SP system, based on the similarity of structures. Nevertheless, results for this system are not as neat as those for SO, because of its lower light stability. These results show the greater sensitivity of Raman experiments to detect changes in the molecular order of the mesogens, compared to birefringence experiments that do not show any change under similar conditions.

The birefringence experiments report the change in the order of the mesophase by the photoconversion. Greater changes in birefringence are induced by the $E \rightarrow Z$ isomerization of NDAB, than by the isomerization of spirocompounds, where changes can only be measured for high conversion. This reflects the higher affinity difference for the mesophase between azobenzene photoisomers than between SP or SO photoisomers. In all cases, the time decay of the birefringence is similar to the time decay of the photoisomer absorption, indicating that the photoisomerization controls the process and that the mesophase rapidly equilibrates with the instantaneous composition of the photochromic system.

In twisted nematic phases, no change in the position of the reflection band could be photoinduced. Slight changes in the transmitted light in the reflection band occurred with similar kinetics as the photochromic transformation, indicating that this process has a small influence in this band. This can be caused by refractive index changes of the nematic layers as those responsible for the birefringence changes, but the high proportion of the chiral inductor governs the pitch of the phase and the photoproduction of achiral compounds or racemic mixtures of them do not perturb the chiral order of the phase.

In summary, for all the systems studied in this work, we show that the order of the mesophase can be changed by light irradiation in both directions. SP turned out to be an interesting photochemical probe as it has orientation photochromism and is able to adequately sense the orientation dependent polarity of this anisotropic medium. Furthermore, the kinetic parameters of the thermal decay of its MC form are very sensitive to medium order.

Acknowledgment. M.L.B. was a Research Fellow from Universidad de Buenos Aires. P.F.A. is member of Carrera del Investigador Científico from CONICET (Consejo Nacional de

Investigaciones Científicas y Técnicas, National Research Council of Argentina). The work was performed under financial support from grants from Fundación Antorchas (Argentina), ANPCyT (Argentina) (Grant Nos. PICT06-4438 and 06-10621), UBA (Grant No. X086), and CONICET (Argentina) (Grant No. PIP 0388). We thank Prof. Peter Hildebrandt for constant support and helpful discussions and David von Stetten for performing some of the Raman measurements.

References and Notes

- (1) Gray, G. W., Ed. *Thermotropic Liquid Crystals*; Wiley: Chichester, U.K., 1987.
- (2) Rosenhauer, R.; Fischer, Th.; Stumpe, J.; Giménez, R.; Piñol, M.; Serrano, J. L.; Viñuales, A.; Broer, D. *Macromolecules* **2005**, *38*, 2213.
- (3) Lee, H.-K.; Doi, K.; Harada, H.; Tsutsumi, O.; Kanazawa, A.; Shiono, T.; Ikeda, T. *J. Phys. Chem. B* **2000**, *104*, 7023.
- (4) Feringa, B. L.; Huck, N. P. M.; van Doren, H. A. *J. Am. Chem. Soc.* **1995**, *117*, 9929.
- (5) Janicki, S. Z.; Schuster, G. B. *J. Am. Chem. Soc.* **1995**, *117*, 8524.
- (6) Tsutsumi, O.; Shiono, T.; Ikeda, T.; Galli, G. *J. Phys. Chem. B* **1997**, *101*, 1332.
- (7) Seki, T.; Tamaki, T.; Suzuki, Y.; Kawanishi, Y.; Ichimura, K.; Aoki, K. *Macromolecules* **1989**, *22*, 3505.
- (8) Vlahakis, J. Z.; Wand, M. D.; Lemieux, R. P. *J. Am. Chem. Soc.* **2003**, *125*, 6862.
- (9) Maly, K. E.; Zhang, P.; Wand, M. D.; Bunzel, E.; Lemieux, R. P. *J. Mater. Chem.* **2004**, *14*, 2806.
- (10) Ikeda, T. *J. Mater. Chem.* **2003**, *13*, 2037.
- (11) Shishido, A.; Tsutsumi, O.; Kanazawa, A.; Shiono, T.; Ikeda, T.; Tamai, N. *J. Am. Chem. Soc.* **1997**, *119*, 7791.
- (12) Ichimura, K. *Chem. Rev.* **2000**, *100*, 1847.
- (13) Ho, M.-S.; Natansohn, A.; Rochon, P. *Macromolecules* **1996**, *29*, 44.
- (14) van Delden, R. A.; Mecca, T.; Rosini, C.; Feringa, B. L. *Chem.—Eur. J.* **2004**, *10*, 61.
- (15) Dürr, H.; Bouas-Laurent, H., Eds. *Photochromism. Molecules and Systems*; Elsevier: Amsterdam, 1990.
- (16) Crano, J. C.; Guglielmetti, R. J., Eds. *Organic Photochromic and Thermochromic Compounds*. Kluwer Academic: Plenum Publishers: New York, 1999.
- (17) See the thematic issue on “Photochromism: Memories and Switches”, *Chem. Rev.* **2000**, *100*, 1683.
- (18) Kurihara, S.; Nomiyama, S.; Nonaka, T. *Chem. Mater.* **2000**, *12*, 9.
- (19) Bobrovsky, A. Y.; Boiko, N. I.; Shibaev, V. P.; Springer, J. *Adv. Mater.* **2000**, *12*, 1180.
- (20) Bobrovsky, A. Y.; Pakhomov, A. A.; Zhu, X.-M.; Boiko, N. I.; Shibaev, V. P.; Stumpe, J. *J. Phys. Chem. B* **2002**, *106*, 540.
- (21) Rau, H. *Azo Compounds in Photochromism. Molecules and Systems*; Dürr, H., Bouas-Laurent, H., Eds.; Elsevier: Amsterdam, 1990.
- (22) Hirose, Y.; Yui, H.; Sawada, T. *J. Phys. Chem. A* **2002**, *106*, 3067.
- (23) Wildes, P. D.; Pacifici, J. G.; Irick, G., Jr.; Whitten, D. G. *J. Am. Chem. Soc.* **1971**, *93*, 2004.
- (24) Nishimura, N.; Sueyoshi, T.; Yamanaka, H.; Imai, E.; Yamamoto, S.; Hasegawa, S. *Bull. Chem. Soc. Jpn.* **1976**, *49*, 1381.
- (25) Guglielmetti, R. *4n + 2 Systems: Spiropyrans in Photochromism. Molecules and Systems*; Dürr, H., Bouas-Laurent, H., Eds.; Elsevier: Amsterdam, 1990.
- (26) Bertelson, R. C. *Spiropyrans. In Organic Photochromic and Thermochromic Compounds*; Crano, J. C., Guglielmetti, R., Eds.; Kluwer Academic/Plenum Publishers: New York, 1999; Vol. 1: Main Photochromic Families.
- (27) Berkovic, G.; Krongauz, V.; Weiss, V. *Chem. Rev.* **2000**, *100*, 1741.
- (28) Seki, T.; Ichimura, K. *J. Colloid Interface Sci.* **1989**, *129*, 353.
- (29) Sueishi, Y.; Ohcho, M.; Nishimura, N. *Bull. Chem. Soc. Jpn.* **1985**, *58*, 2608.
- (30) Sueishi, Y.; Ohcho, M.; Yamamoto, S.; Nishimura, N. *Bull. Chem. Soc. Jpn.* **1986**, *59*, 3666.
- (31) Value supplied by the manufacturer.
- (32) Bossi, M.; Aramendía, P. F. *Photochem. Photobiol. Sci.* **2002**, *1*, 507.
- (33) Favaro, G.; Malatesta, V.; Mazzucato, U.; Ottavi, G.; Romani, A. *J. Photochem. Photobiol. A: Chem.* **1995**, *87*, 235.
- (34) Favaro, G.; Ortica, F.; Malatesta, V. *J. Chem. Soc., Faraday Trans.* **1995**, *91*, 4099.
- (35) Yakovenko, S. Ye. *Liq. Cryst.* **1999**, *26*, 23.
- (36) Joo, S. W.; Chung, T. D.; Jang, W.; Gong, M.-S.; Geum, N.; Kim, K.; *Langmuir* **2002**, *18*, 8813.
- (37) Davies, A. N.; Jones, W. J.; Price, A. H. *J. Raman Spectrosc.* **1994**, *25*, 521.
- (38) Jones, W. J.; Thomas, D. K.; Thomas, D. W.; Williams, G. *J. Mol. Struct.* **2002**, *614*, 75.
- (39) Wetzler, D. E.; Aramendía, P. F.; Japas, M. L.; Fernández-Prini, R. *Phys. Chem. Chem. Phys.* **1999**, *1*, 4955.
- (40) Bertelson, R. C. *Photochromic Processes Involving Heterolytic Cleavage. In Photochromism*; Brown, G. H., Ed.; Wiley-Interscience: New York, 1971.
- (41) Asan, T.; Okada, T. *J. Org. Chem.* **1984**, *49*, 4387.
- (42) Literature data are obtained from refs 23, 24, and 40. A different correlation is observed for protic solvents such as formamide, 2-propanol, ethanol, or methanol.
- (43) Reichardt, C. *Chem. Rev.* **1994**, *94*, 2319.
- (44) Asano, T.; Okada, T.; Shinkai, S.; Shigematsu, K.; Kusano, Y.; Manabe, O. *J. Am. Chem. Soc.* **1981**, *103*, 5161.
- (45) No experiments were conducted at higher temperatures, because the time needed to photolyze the sample becomes comparable with the decay time of the photoisomer.
- (46) Otruba, J. P., III; Weiss, R. G. *J. Org. Chem.* **1983**, *48*, 3448.
- (47) Krug, R. R.; Hunter, W. G.; Grieger, R. A. *J. Phys. Chem.* **1976**, *80*, 2335.
- (48) Favaro, G.; Masetti, F.; Mazzucato, U.; Ottavi, G.; Allegrini, P.; Malatesta, V. *J. Chem. Soc., Faraday Trans.* **1994**, *90*, 333.
- (49) Maeda, S. *Spirooxazines. In Organic Photochromic and Thermochromic Compounds*; Crano, J. C., Guglielmetti, R., Eds.; Kluwer Academic/Plenum Publishers: New York, 1999; Vol. 1: Main Photochromic Families.
- (50) Kapko, V.; Matyushov, D. V. *J. Chem. Phys.* **2006**, *124*, Article No. 114904.
- (51) For the relationship between orientation factors of the transition moments and molecular axes, see Michl, J.; Thulstrup, E. W. *Spectroscopy with Polarized Light*; VCH Publishers: New York, 1995.
- (52) Flannery, J., Jr. *J. Am. Chem. Soc.* **1968**, *90*, 5660.